Air Return Ratio Measurements at the Solar Tower Jülich using a Tracer Gas Method

Arne Tiddens[a,*], Marc Röger[b], Hannes Stadler[a], Bernhard Hoffschmidt[c]

[a] *Institute of Solar Research, German Aerospace Center (DLR), Karl-Heinz-Beckurts-Str.13, 52428 Jülich, Germany*
[b] *Institute of Solar Research, German Aerospace Center (DLR), Plataforma Solar de Almería, Tabernas 04200, Spain*
[c] *Institute of Solar Research, German Aerospace Center (DLR), Linder Hoehe, 51147 Cologne, Germany*

Abstract

The air return ratio is a key factor for the overall efficiency of the open volumetric receiver concept. Although first measurements of the air return ratio exist for smaller setups of the open volumetric receiver concept, so far no measurement of the air return ratio has been presented for the Solar Thermal Test and Demonstration Power Plant Jülich ($\approx 1.5\,\mathrm{MW}$, $\approx 10\,(\mathrm{kg\ air})/\mathrm{s}$; $\approx 700\,^{\circ}\mathrm{C}$). This paper describes the application of a tracer gas method at the Solar Tower Jülich to determine this substantial ARR.
As tracer gas the environmentally friendly helium has been chosen. The helium is injected dynamically into the circular air flow of the system and the helium mole fraction is measured using a mass spectrometer. The dynamic concentration response of the system is used to determine the air return ratio. This dynamic method only requires one location of measurement. First measurements with this dynamic method were conducted at the Solar Tower Jülich. The ARR of STJ was measured with and without irradiation of the main receiver with high accuracy.

Under low-wind conditions and without irradiation of the main receiver the air return ratio was measured to be $(67.7 \pm 0.5)\,\%$ for an air mass flow of $(9.96 \pm 0.04)\,\mathrm{kg/s}$. A slightly higher air return ratio of $(68.6 \pm 0.7)\,\%$ was measured under irradiation with an air mass flow of $(9.94 \pm 0.04)\,\mathrm{kg/s}$. The air return ratio was sensitive to the air mass flow, showing significantly lower rates when moving further away from the $10\,\mathrm{kg/s}$ design air mass flow to $5\,\mathrm{kg/s}$.

Keywords: Air return ratio, Tracer gas, Solar Tower Jülich, Solar air receiver, Air receiver, Measurement technique, Dynamic mass spectroscopy

1. Motivation and Background

Concentrated solar power provides an environmentally friendly and virtually unlimited source of high-temperature heat [9]. This heat can be converted into electricity, stored or used as process heat for industrial processes. Since this process heat can be stored, concentrated solar power is considered to be a stable renewable energy source.

The heat is generated by concentrating sunlight using mirrors onto a solar receiver where the radiant energy is absorbed and transformed into thermal energy. This energy can be transported using various heat transfer fluids and can be stored until further use. Central receiver systems have a high potential due to an increase in the achieved temperature [9]. Additionally, central receiver plants are the most resource-efficient ones [10]. The commonly used thermal fluids in the receiver are saturated or superheated steam and nitrate-based molten salts. In the volumetric receiver concept the irradiation is volumetrically absorbed. This concept could allow a more efficient solar energy capture and conversion. [9]

It was realized at the solar tower Juelich (STJ) in 2008 with a field of 2153 heliostats. These reflect and concentrate the sunlight onto an open volumetric receiver at the top of the 60 meter high solar tower power plant. The receiver consists of a porous ceramic structure of modular design to allow for scalability. It comprises of 1080 absorber modules (see Fig. 1B) which make up the receiver (see Fig. 1C). By absorbing the sunlight the front of this receiver is heated to around $700\,^{\circ}\mathrm{C}$ [2]. As heat transfer fluid air is sucked through the absorber modules to transport the thermal energy to a heat exchanger or storage unit. Due to the low heat capacity of air, high air mass flows are required.

To increase efficiency a fraction of the blown out air is sucked in again. This fraction is the substantial air return ratio (ARR) which is defined by Ahlbrink et al. [1] as

$$ARR = \frac{\dot{m}_{\mathrm{return}}}{\dot{m}_{\mathrm{out}}}\,. \tag{1}$$

Hereby $\dot{m}_{\mathrm{out}}$ is the air mass flow blown out in between the absorber cups, and $\dot{m}_{\mathrm{return}}$ is the part of this air which

*Corresponding author
Email address: Arne.Tiddens@dlr.de (Arne Tiddens)

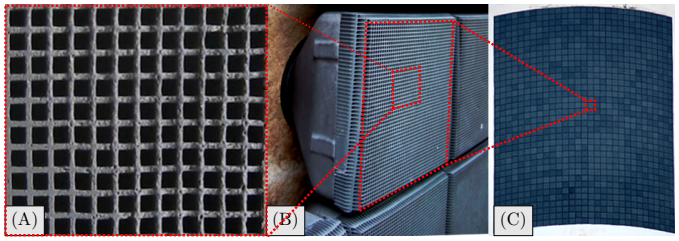

Figure 1: The receiver of the solar tower Juelich. (A) shows a close up of the absorber structure of the Hitrec-II absorber module, (B) individual absorber modules during maintenance which make up the main receiver of the solar tower Juelich (C).

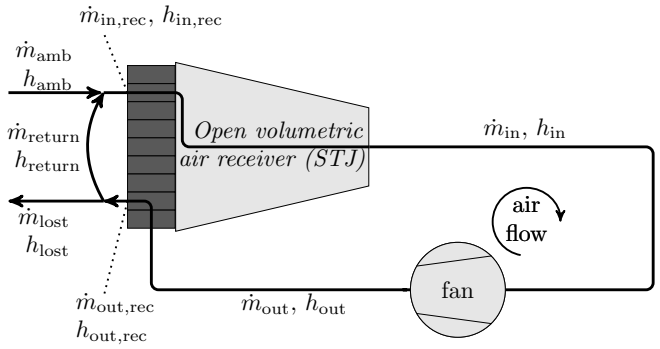

Figure 2: A schematic of the open volumetric receiver is shown. The air mass flows $\dot{m}$ and specific enthalpies h are indicated.

is sucked in again into the air circuit. Ideally, the ARR would be 100 %. In addition to the substantial ARR Maldonado Quinto [8] defines a thermal ARR at the receiver surface as

$$ARR_{\mathrm{thermal}} = \frac{\dot{m}_{\mathrm{in,rec}} \cdot (h_{\mathrm{in,rec}} - h_{\mathrm{amb}})}{\dot{m}_{\mathrm{out,rec}} \cdot (h_{\mathrm{out,rec}} - h_{\mathrm{amb}})}\,, \qquad (2)$$

whereby $h_{\mathrm{out,rec}}$ is the specific enthalpy of the blown out air, $h_{\mathrm{in,rec}}$ of the sucked in air and h_{amb} of the ambient air. The reason for defining ARR_{thermal} is to calculate the overall efficiency of the power plant. A schematic of the air flow within the receiver is shown in Fig. 2. The points at which the above used enthalpies are defined, are indicated. The thermal ARR and hence especially the specific enthalpies and mass flows are defined at the surface of the receiver. If the small losses of the return air enthalpy due to conduction and gas emission of air are neglected, the thermal ARR turns into the substantial ARR (Eq. 1) [8]. The measurement of this substantial ARR is discussed within this paper.

To improve the receiver efficiency it is important to increase the ARR and therefore minimize the occurring leak within the air circuit. At an receiver air output temperature of 650 °C an improvement from an $ARR = 60\,\%$ to $ARR = 80\,\%$ causes an increase in 8 percentage points of the normalized system efficiency [8]. The ARR is so far unknown on a large scale and under solar irradiation. Since it can be influenced by a multitude of measures as for

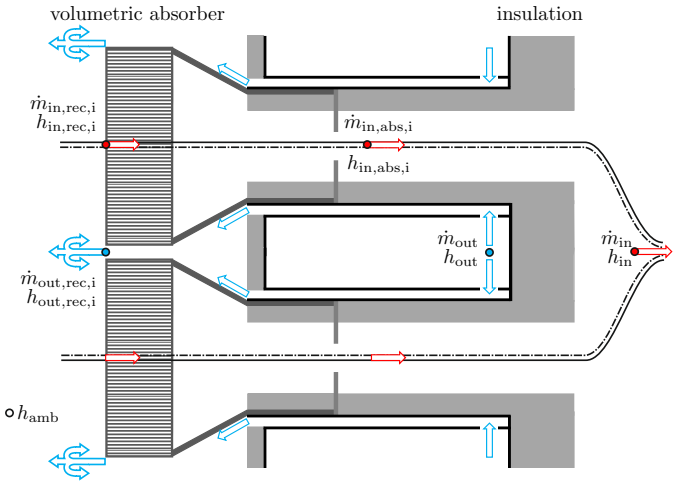

Figure 3: A schematic of the air flow within the open volumetric air receiver is shown. Based on Ahlbrink et al. [1].

example wind speed and direction, it is of vital importance to be able to measure it [15, 14].

2. State of the Art

The development of open volumetric receivers and an overview of measured ARR are given in full by Ávila-Marín [3]. ARR measurements can be conducted by either measuring at the receiver front, or by measuring within the air system.

The most useful ARR measurement for predicting power plant efficiency would be the direct measurement of the thermal ARR_{thermal} according to Eq. 2. To achieve this it would be necessary to measure the complete flow field at the receiver surface ($\dot{m}_{\mathrm{out,rec,i}}$, $\dot{m}_{\mathrm{in,rec,i}}$) and the temperatures of all air flows at the receiver front to determine $h_{\mathrm{out,rec,i}}$ and $h_{\mathrm{in,rec,i}}$.

The air flow field in front of the receiver would have to be measured with very high precision. However, most flow measurement techniques can not be employed on the large-scale of solar tower power plants or do not yield quantitative results. The most feasible flow measurement technique is the laser based Particle Image Velocimetry (PIV). It could be applied on such a scale, but the large resulting measurement uncertainties would render the ARR results useless. To measure the flow field locally would require thousands of mass flow measurements. The temperatures of all air flows could also only be measured locally with thousands of thermocouples. Since the receiver front is additionally exposed to highly concentrated solar radiation, this is not realistic.

Instead of measuring the air mass flows and temperatures at the receiver front it could be measured within the air circuit. Assuming that $h_{\mathrm{in,rec}} = h_{\mathrm{in}}$, $h_{\mathrm{out,rec}} = h_{\mathrm{out}}$, a constant specific heat capacity of air and that $\dot{m}_{\mathrm{in}} = \dot{m}_{\mathrm{out}}$

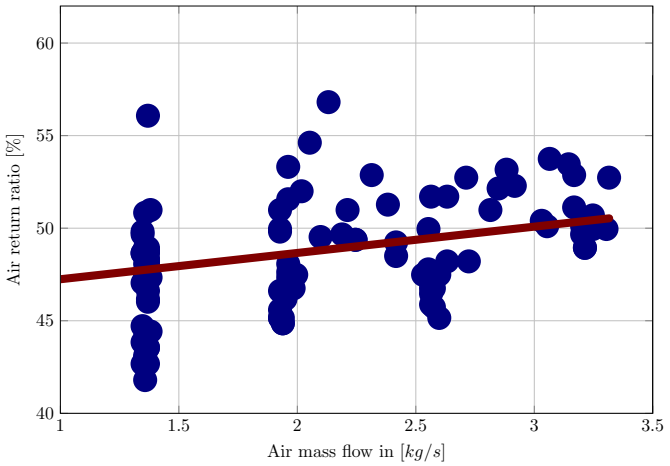

Figure 4: ARR measurement results at the SOLAIR 3000 receiver. These measurements should only be seen as a rough estimate (see Eq. 4). Based on [12]

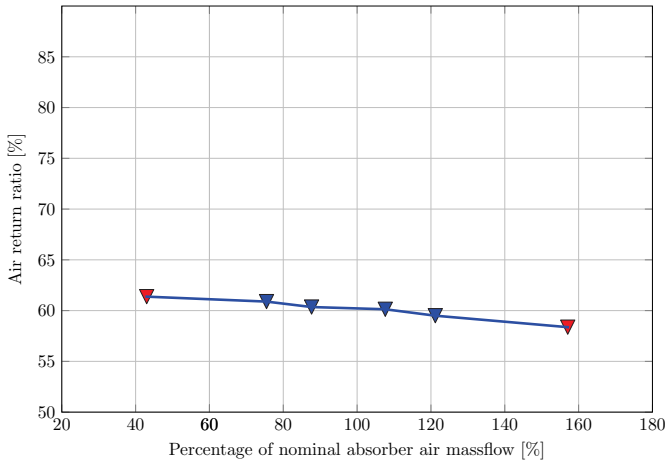

Figure 5: Simulated ARR of one absorber module for different percentages of the nominal air mass flux. The ARR decreases only very slightly with increasing mass flow of the system. Maldonado Quinto [8]

Eq. 2 could be expressed as

$$ARR_{\text{thermal}} = \frac{T_{\text{in,rec}} - T_{\text{amb}}}{T_{\text{out,rec}} - T_{\text{amb}}} \,. \tag{3}$$

This is consistent with definition of Hoffschmidt et al. [6]. An ARR measurement based on temperature measurements within the air circuit has also been conducted by Téllez et al. [12] at the SOLAIR 3000 receiver. These measurements were performed without solar radiation. The ARR results are shown in Fig. 4 for various air mass flows.

This however is not correct since the enthalpy of the sucked in air at the receiver surface ($h_{\text{in,rec,i}}$) is different from the enthalpy of the air at the absorber outlet ($h_{\text{in,abs,i}}$) and the receiver outlet (h_{in}). This results from the heat transfer between the sucked in and blown out air within the receiver [1] leading to

$$\begin{aligned} ARR_{\text{thermal}} &= \frac{\dot{m}_{\text{in,rec}} \cdot (h_{\text{in,rec}} - h_{\text{amb}})}{\dot{m}_{\text{out,rec}} \cdot (h_{\text{out,rec}} - h_{\text{amb}})} \\ &\neq \frac{\dot{m}_{\text{in}} \cdot (h_{\text{in}} - h_{\text{amb}})}{\dot{m}_{\text{out}} \cdot (h_{\text{out}} - h_{\text{amb}})} \,. \end{aligned} \tag{4}$$

The temperature and flow measurements therefore have to be conducted at the receiver surface with a high spatial resolution. As this is not feasible direct measurements of ARR_{thermal} are impossible.

When the receiver is irradiated by solar radiation the heat transfer between the sucked in and blown out air within the receiver becomes even more prominent. Téllez et al. [12] however determine h_{in} using a weighted average of $h_{\text{in,abs,i}}$ without measuring the air mass flows $\dot{m}_{\text{in,rec,i}}$. The results shown in Fig. 4 should hence only be considered a very rough estimate.

The absence of a reliable ARR reference measurement causes computational fluid dynamics (CFD) simulations to be the most important reference. CFD simulations have been conducted and validated using PIV for a model containing one absorber module by Maldonado Quinto [8]. This model was used to calculate the ARR for an irradiated and undisturbed absorber module for various air mass flows, depicted in Fig. 5.

The simulation boundary conditions are described in [8]. The ARR of the examined system decreases only very slightly with increasing mass flow of the system.

3. Theory of ARR Measurements

Due to the difficulties measuring ARR_{thermal}, a tracer gas method was used to determine the substantial ARR. Hereby the tracer gas helium is injected and measured in the air flow of the STJ. The development, the validation and the necessary correction functions of the developed tracer gas method are described in more detail in [13].

The injected helium mass flow is small compared to the air mass flow. Therefore the molar mass of all examined air flows can be considered equal ($M_{\text{return}} \approx M_{\text{out}} \approx M_{\text{amb}}$). The ARR can hence be written as

$$ARR = \frac{\dot{m}_{\text{return}}}{\dot{m}_{\text{out}}} = \frac{\dot{n}_{\text{return}}}{\dot{n}_{\text{out}}} \cdot \underbrace{\frac{M_{\text{return}}}{M_{\text{out}}}}_{\approx 1} \,, \tag{5}$$

with $\dot{n}_{\text{return}}$ and $\dot{n}_{\text{out}}$ being the molar mass flow of the return air and blown out air, respectively.

Furthermore it can approximated that $\dot{n}_{\text{out}} = \dot{n}_{\text{in}}$. Therefore the mass of air which is stored within the air system can not change significantly in comparison to the examined air mass flow within the investigated time frame. Since this is the case at the STJ and the added helium mass flow is furthermore negligible, the approximation is considered justified.

Fig. 6 depicts a schematic of the air circuit of the STJ with the occurring molar mass flows and molar fractions.

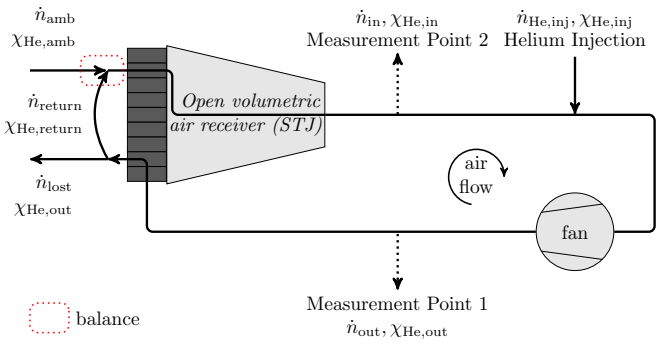

Figure 6: Schematic diagram of the air circuit of the STJ. Based on Tiddens et al. [13].

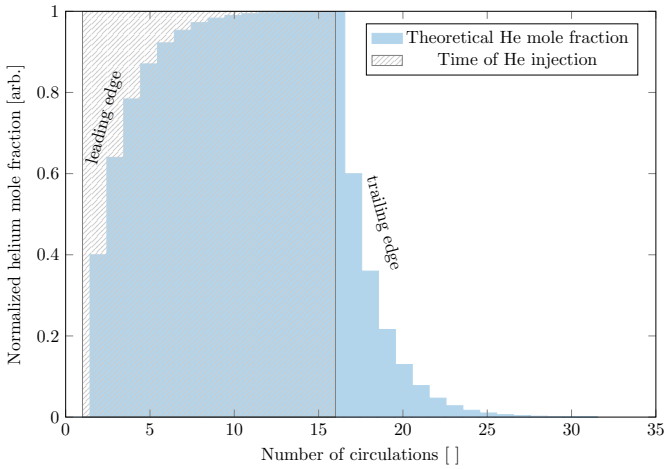

Figure 7: The theoretical helium mole fraction response to a helium injecting with a fixed flow rate and duration is shown for a circular air circuit with $ARR = 0.6$. The dispersion of helium in the system is ignored. Based on Tiddens et al. [13].

The indicated mole balance combined with $\dot{n}_{out} = \dot{n}_{in}$ leads to

$$\dot{n}_{return} + \dot{n}_{amb} = \dot{n}_{in} = \dot{n}_{out}\,. \tag{6}$$

When regarding the same mole balance for helium it can be expressed as

$$\dot{n}_{return} \cdot \chi_{He,return} + \dot{n}_{amb} \cdot \chi_{He,amb} = \dot{n}_{in} \cdot \chi_{He,in} \tag{7}$$

with χ_{He} being the helium mole fraction at different places in the air circuit.

The mixing of return and ambient that occurs in front of the receiver is turbulent and therefore the dispersion is much faster than the diffusion. This arises from the different origin of dispersion and diffusion in turbulent flow. Whereas diffusion is caused by the small-scale Brownian motion, the turbulent dispersion is caused by gusts and eddies [4]. Therefore, the diffusion of helium away from the return air towards the ambient can neglected and it can be assumed that $\chi_{He,return}$ is equal to $\chi_{He,out}$.

With Eqs. 6 and 7 this results in

$$\underbrace{\frac{\dot{n}_{return}}{\dot{n}_{out}}}_{=ARR} \cdot \chi_{He,out} + (1 - \underbrace{\frac{\dot{n}_{return}}{\dot{n}_{out}}}_{=ARR}) \cdot \chi_{He,amb} = \chi_{He,in}\,. \tag{8}$$

Combined with Eq. 5, the ARR can be written as

$$ARR = \frac{\chi_{He,in} - \chi_{He,amb}}{\chi_{He,out} - \chi_{He,amb}}\,. \tag{9}$$

By measuring $\chi_{He,in}$, $\chi_{He,out}$ and $\chi_{He,amb}$ the ARR can be calculated, as long as $\chi_{He,out} \neq \chi_{He,amb}$. Helium must be injected into the system to achieve this. The locations of this injection and of the mole fraction measurement are hereby chosen in a way, to assure that both of the following described measurement techniques can be applied. The injection location furthermore improves the mixing of the injected helium by the fan before the next measurement point (see Fig. 6).

3.1. Static ARR Measurement

The simplest method to determine the ARR is to inject the tracer gas as shown in Fig. 6. The tracer mole fractions $\chi_{He,out}$ and $\chi_{He,in}$ are measured at measuring point 1 and 2, respectively. Combined with the ambient helium mole fraction $\chi_{He,amb}$ the ARR can be calculated by applying Eq. 9. Before measuring the ARR, it has to be examined if the helium mole fraction distribution across the cross section of the piping at both measuring points is homogeneous. This is necessary to allow single point sampling and is therefore a prerequisite of the static tracer gas measurement. For the static ARR measuring method two measuring points with homogeneous tracer distributions are required. This could be difficult at the STJ for measuring point 2, since it can only be located very close to the receiver. Therefore, the homogeneity of the tracer within the air circuit at this point is uncertain and has to be confirmed by measurement (see Sec. 6).

3.2. Dynamic ARR Measurement

Since the air system is of a circular nature, it is possible to determine the ARR using only one measuring point when measuring dynamically. Helium is therefore injected with a fixed flow rate and duration into the air system. The resulting helium mole fraction response over time is measured at measuring point 1. For the static measurement the helium mole fraction is measured at equilibrium. In contrast to this, the transient mole fraction curves are considered and the entire mole fraction curve is fitted for the dynamic measurement. The chosen measuring point 1 is located directly behind the blower. Here the mole fraction of helium across the cross section of the piping is most likely homogeneous. The disadvantage of the dynamic measuring method is that its measurement procedure and the evaluation of the data is more complex compared to the static measurement. In Fig. 7 the theoretical mole fraction response to a helium injection with a fixed flow rate and duration is shown if dispersion of helium is ignored. The helium mole fraction of the leading edge increases until its

maximum is reached at equilibrium. The trailing edge is caused by the end of helium injection. The helium mole fraction decreases every period length T_{circ} by the factor ARR. The distinguished mole fraction steps in Fig. 7 disappear during measurement due to dispersion. The trailing curve can be described by

$$\chi_{\mathrm{He,trailing,norm}}(t) = ARR^{t/T_{\mathrm{circ}}}\,, \tag{10}$$

since every circulation period the helium mole fraction is reduced by the factor ARR. Both leading and trailing edge must have the same amplitude A. Additionally, the helium mole fraction of the leading edge is increasing with the same ARR as the trailing edge. The helium mole fraction response of the leading edge can hence be described by the following exponential growth function

$$\chi_{\mathrm{He,leading}}(t) = A(1 - (ARR)^{t/T_{\mathrm{circ}}})\,. \tag{11}$$

To determine the ARR, the functions of the leading and trailing edge must be fitted to the measurement data, with the ARR as the only unknown parameter in Eqs. 10 and 11. To achieve this, first the amplitude is removed by normalization. Furthermore, the circulation period T_{circ} must be measured. It can be measured by injecting helium with a short duration into the air circuit and measuring the helium mole fraction response. The time between two measured mole fraction peaks caused by the same injected helium, is the circulation period. Since measuring dynamically, the dynamic error of the measurement setup must corrected for. This is necessary since the measurement setup does not have an ideal transfer function. The dynamic error is corrected by multiplying the measured ARR with the dynamic error correction term cor_{dyn}. This correction term is described in detail in [13].

4. Solar Tower Juelich

The Solar Thermal Test and Demonstration Power Plant Juelich (STJ) was built as a demonstration as well as research power plant in 2008 by a consortium consisting of the German Aerospace Center (DLR), Solar Institute Jülich, Kraftanlagen München GmbH and Stadtwerke Jülich. It was taken over by the DLR in 2011.[7] In Fig. 8 a photo of the 60 meters high solar power tower is depicted. The main receiver (A) as well as the Testreceiver (C) can be seen. These two receivers can be irradiated by reflecting and concentrating sunlight with 2153 heliostats onto their surface. The heliostats make up a combined total surface of nearly 18000 m^2 [5]. Their back structure can be seen in (D).

The main receiver covers a surface area of around 22 m^2. It has the shape of a section of a cylinder and is inclined downwards towards the heliostats. It consists of 1080 ceramic absorber modules through which air is sucked in and heated to a temperature of about 680 °C. This hot air can be sucked through the thermal storage system consisting of

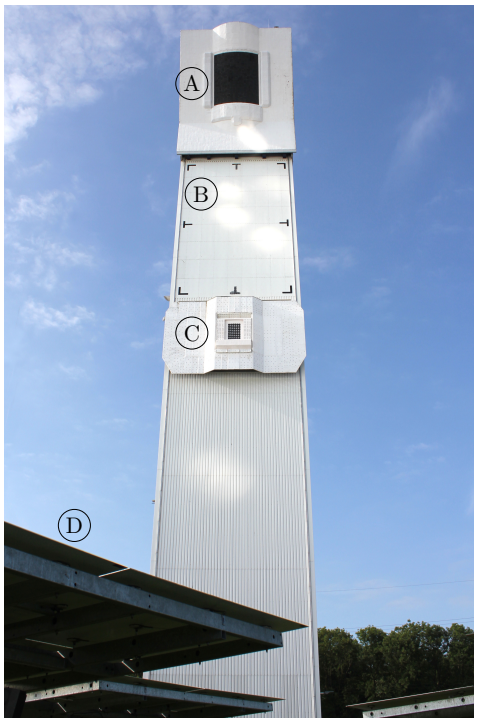

Figure 8: Photo of the STJ displaying the main receiver (A) at the top, the target for the calibration of heliostats (B), the Testreceiver (C) and the heliostats (D) at ground level.

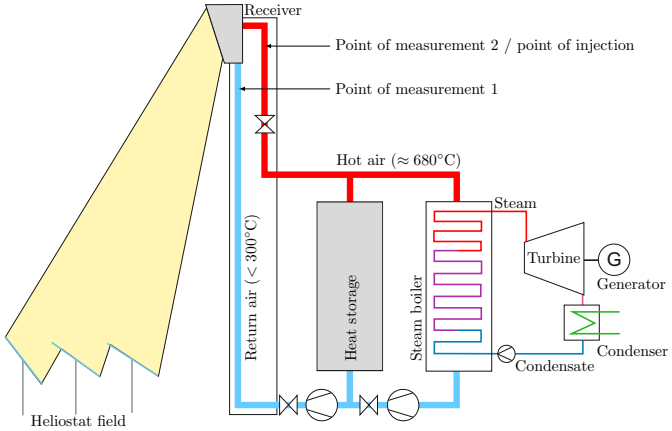

Figure 9: Schematic of the STJ. Air is sucked through the irradiated receiver, heating up to about 680 °C. It is used to drive a water steam cycle or to heat up a thermal storage. The still warm air (< 300 °C) is returned to the receiver front to increase efficiency. The location of the helium mole fraction measuring points and helium injection are indicated. [DLR]

a large vessel filled with porous ceramic bricks or directly through the steam boiler. The steam is generated in a heating tube boiler, which is further used to drive a turbine and produce electricity [7]. After passing the thermal storage or the steam boiler, the air is returned to the receiver front. Here it is blown out through the gaps between the absorber modules. This is depicted schematically in Fig. 3.

A schematic summary of the functionality of the STJ is shown in Fig. 9.

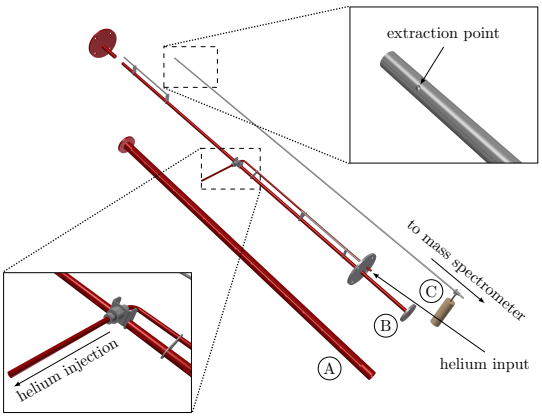

Figure 10: Schematic of the measurement probe at measuring point 2 which incorporates the injection of helium. The inner probe (A) is held in place by its support structure (B,C). By moving this inner probe a sample can be extracted towards the mass spectrometer at discrete locations along the cross section of the piping of the STJ.

For the ARR measurements the STJ has been operated in a mass flow controlled mode. The air mass flow is measured using an ultrasonic flow meter (GE Sensing, Digital Flow) and controlled varying the speed of the fan. Since the STJ is mainly designed for research, a large number of thermocouples measure the temperature within the air circuit of the STJ.

5. Setup

To measure the helium mole fraction at the measuring points, gas samples must be extracted. Probes have been constructed and built allowing the extraction and the measurement of the helium mole fraction distribution along the cross section of the piping. By moving the inner probe within its support structure, the position of the opening of the probe can be moved to discrete locations along the cross section of the piping of the STJ. This is necessary to determine if point sampling at the measuring point is adequate. The helium injection was incorporated into the measuring probe at measuring point 2 which is shown in Fig. 10. In Fig. 11 the probe shown in Fig. 10 can be seen in an assembled state (red probe) within the piping of the STJ. The setup allows air/helium samples to be extracted at 30 discrete measurement locations along the crosssection of the piping at both measuring points. The location of sample extraction can be altered during operation of the power plant. The helium injection is facing away from the extraction probes in the direction of the air flow. The probes furthermore include mounts for the thermocouples (D). The inner insulation of the piping of the STJ is not shown.

6. Results

To verify if the tracer gas measurements are suitable for the application at the STJ first the homogeneity of the tracer gas has to be examined.

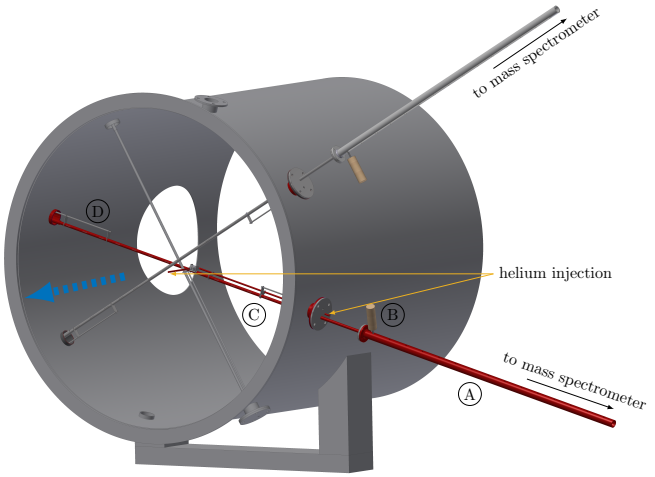

Figure 11: Schematic of the measuring point 2, with both measurement probes. The red probe (see Fig. 10) furthermore incorporates the downstream (blue arrow) helium injection. The probes furthermore include mounts for the previously installed thermocouples (D).

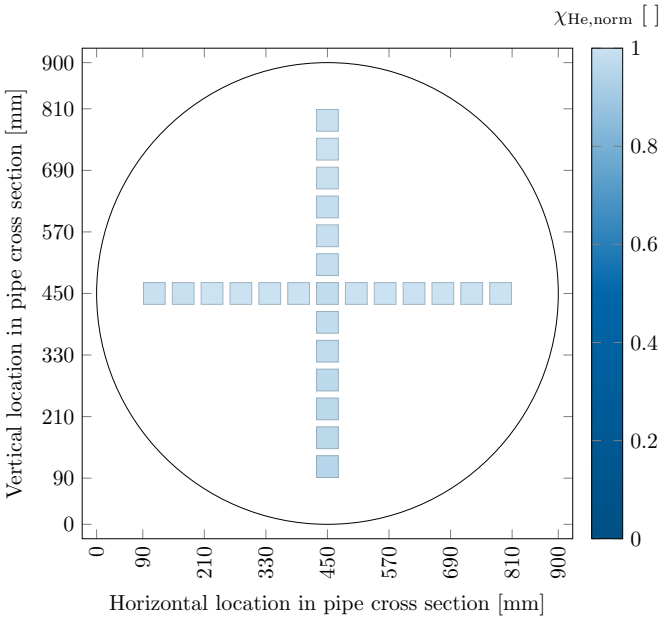

Figure 12: The helium mole fraction along the cross section of the piping of the STJ at measuring point 1 is shown. These measurements were performed with an ARR of zero. The measurements show only minor fluctuations, with a standard deviation of 1.4 %.

6.1. Homogeneity at Measuring Points

To examine the homogeneity at measuring point 1 a measurement with an ARR of zero was conducted. This was achieved by blowing the air out through a vent in the STJ which is located between the measuring point 1 and the receiver. Only small deviations of the mean ARR of 1.4 % were found (see Fig. 12). Therefore, a centrally extracted mole fraction represents the mean of the cross section, allowing point sampling. The measurements at measuring point 2 shown in Fig. 13 however show large fluctuations

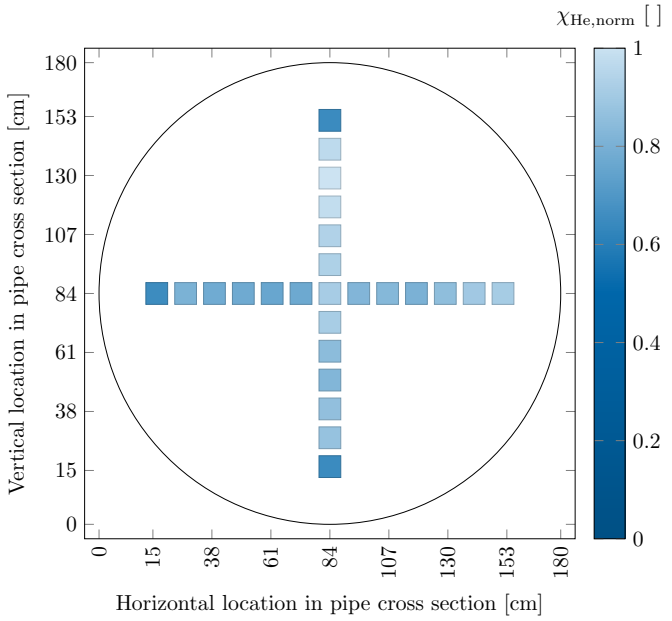

Figure 13: The helium mole fraction along the cross section of the piping of the STJ at measuring point 2 is shown. Large fluctuations with a standard deviation of 9.7 % are observed. This inhibits single point sampling at measuring point 1, rendering the static method inapplicable.

with a standard deviation of 9.7 %. The static measurement however requires a homogeneous helium distribution across the piping at both measuring points, and hence cannot be applied at the STJ. The static measurement was used to validate the dynamic method which is covered in [13]. Since the dynamic method only requires one measurement point it can be applied at the STJ. Before each ARR measurement, the circulation period must be measured, as it changes with the air mass flow.

6.2. Circulation Period

To determine the circulation period, helium was injected into the air system of the STJ. It was found that an injection time of 10 s results in the strongest signal to noise ratio. It was therefore measured for each ARR measurement individually.

Figures 14 and 15 show the helium mole fraction of two circulation period measurements. The measurements were performed at an air mass flow of 5 kg/s and 10 kg/s, respectively. The two shown exemplary measurements were conducted without irradiation of the receiver. The circulation period was found to be $T_{\mathrm{circ}} = (52.5 \pm 2.5)\,\mathrm{s}$ and $T_{\mathrm{circ}} = (25.4 \pm 1.4)\,\mathrm{s}$, respectively. All circulation period measurements are conducted for 120 s for evaluation reasons. The duration of 120 s was chosen to enable the passing of two peaks at the lowest examined air mass flow. This is the reason why a third peak can be detected in the helium mole fraction in Fig. 15. Since this peak however has a low signal to noise ratio it is not considered during the calculations.

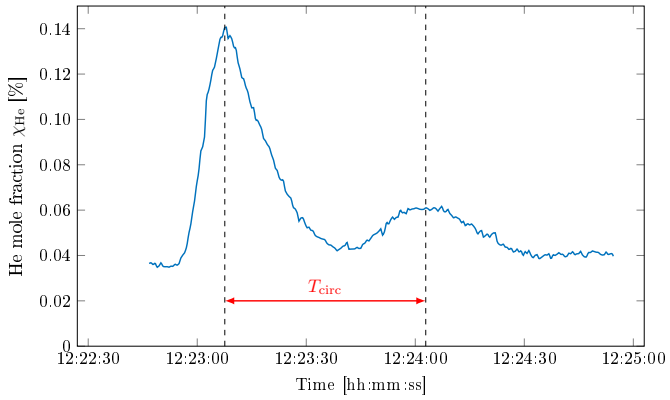

Figure 14: The helium mole fraction of a circulation period measurement at an air mass flow of $\dot{m} = 5\,\mathrm{kg/s}$. A circulation period of $T_{\mathrm{circ}} = (52.5 \pm 2.5)\,\mathrm{s}$ was found by measuring the duration in between the peaks.

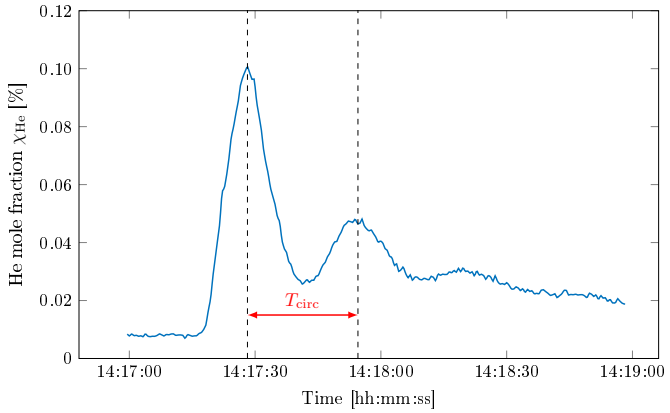

Figure 15: The helium mole fraction of a circulation period measurement at an air mass flow of $\dot{m} = 10\,\mathrm{kg/s}$. A circulation period of $T_{\mathrm{circ}} = (25.4 \pm 1.4)\,\mathrm{s}$ was found by measuring the duration in between the peaks.

The circulation measurement is repeated more often (5 times) than the dynamic measurements (3 times) since the time of 120 s per measurement is short compared to the typical measurement time of the dynamic method.

6.3. Measurements without Irradiation

Figure 16 depicts a typical helium mole fraction curve of the dynamic ARR measurement without the presence of radiation. The trailing and leading edge of this helium mole fraction data is fitted according to Eqs. 10 and 11, respectively. Only small deviations from the measured helium mole fraction data ($\chi_{\mathrm{He,meas,norm}}$) are observed.

The measured values were corrected for the dynamic error of the measurement setup. The corrected values of the $ARR_{\mathrm{meas,dyn}}$ were found to be (51.3 ± 0.8) % and (67.7 ± 0.5) % at air mass flows of $(4.98 \pm 0.03)\,\mathrm{kg/s}$ and $(9.96 \pm 0.04)\,\mathrm{kg/s}$, respectively. The measurements were conducted for an average return air temperature of $(18.0 \pm 1.2)\,^{\circ}\mathrm{C}$ and $(18.9 \pm 0.6)\,^{\circ}\mathrm{C}$. The average wind speed was $(4.8 \pm 2.0)\,\mathrm{m/s}$ and $(3.2 \pm 1.5)\,\mathrm{m/s}$. These results as well as

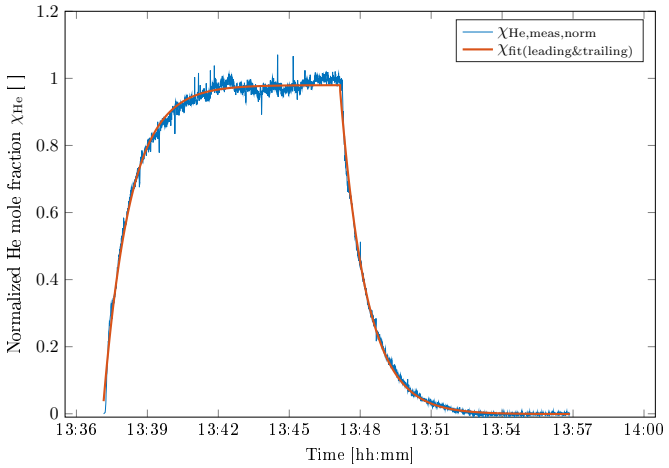

Figure 16: Measured and fitted helium mole fraction of the dynamic method is shown over time. The measurement was conducted without the presence of radiation. It was performed at an air mass flow of (9.96 ± 0.04) kg/s.

Table 1: The ARR results of measurements at the STJ without irradiation for two different air mass flows.

Measured variable	Low air mass flow	High air mass flow
Air mass flow ($\dot{m}$)	(4.98 ± 0.03) kg/s	(9.96 ± 0.04) kg/s
Wind Speed ($v_{\phi,wind}$)	(4.8 ± 2.0) m/s	(3.2 ± 1.5) m/s
Circulation period (T_{circ})	(52.2 ± 0.5) s	(25.5 ± 0.6) s
Measured ARR (ARR_{fit})	(52.5 ± 0.8) %	(68.6 ± 0.5) %
Dynamic correction (cor_{dyn})	(0.979 ± 0.003)	(0.987 ± 0.003)
Corrected ARR (ARR_{dyn})	(51.3 ± 0.8) %	(67.7 ± 0.5) %

the corresponding circulation periods and corrections are shown in Table 1.

6.4. Measurements with Irradiation

The ARR under irradiation of the main receiver was found to be (56.3 ± 1.0) % and (68.6 ± 0.7) % for an air mass flow of (4.96 ± 0.07) kg/s and (9.94 ± 0.04) kg/s, respectively. These measurements were performed at an average return air temperature of (159.6 ± 18.2) °C and (103.6 ± 2.6) °C. An average wind speed of (7.5 ± 2.7) m/s was recorded for the first measurement. No wind data was available for the second measurement. These results are shown in Table 2.

Table 2: The ARR results of measurements at the STJ with irradiation for two different air mass flows.

Measured variable	Low air mass flow	High air mass flow
Air mass flow ($\dot{m}$)	(4.96 ± 0.07) kg/s	(9.94 ± 0.04) kg/s
Circulation period (T_{circ})	(39.0 ± 0.8) s	(23.5 ± 0.5) s
Measured ARR (ARR_{fit})	(57.4 ± 1.0) %	(69.4 ± 0.7) %
Dynamic correction (cor_{dyn})	(0.981 ± 0.003)	(0.988 ± 0.003)
Corrected ARR ($ARR_{meas,dyn}$)	(56.3 ± 1.0) %	(68.6 ± 0.7) %

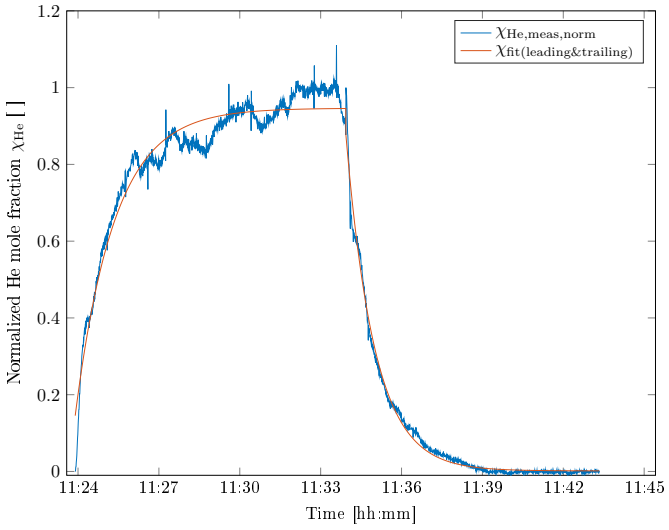

Figure 17: The measured and fitted helium mole fraction of the dynamic method is shown over time. It was conducted with an irradiated receiver at an air mass flow of (4.96 ± 0.07) kg/s. The helium mole fraction data shows large deviations from the fit.

6.5. Fluctuating Air Return Ratio

The difference between the applied fits and the mole fraction curves of the displayed results is very small. However, some measured mole fraction curves measured showed large deviations between the shape of the analytically derived curve. These were conducted at different operational parameters and the ARR results are not presented in this paper. Fig. 17 however shows the helium mole fraction of such a measurement over time with large deviations from the fit. Due to the low temporal resolution of the analytical method, these fluctuations can not be resolved. A method in which the ARR for each individual helium mole fraction data point is calculated numerically could in future allow a higher temporal resolution.

7. Discussion and Conclusion

The main goal of this paper is the measurement of the ARR at the STJ. The ARR depends on many variables such as wind, geometry of the receiver design and operational mode. The ARR of the STJ was prior to this work unknown.

The STJ is a difficult measurement environment due to surface temperatures of up to 1000 °C and large open air mass flows of around 10 kg/s.

The thermal ARR is not directly measurable, because all necessary temperature and flow measurements would have to be conducted at the surface of the receiver with a high spatial resolution. Instead the substantial ARR is measured within this paper. This is possible since the return air flow in front of the receiver is turbulent. Therefore the diffusion of helium and thermal conduction effects become negligible. The substantial ARR can hence be assumed to be equal to the thermal ARR.

To achieve this, it was decided to use a tracer gas method. Hereby the environmentally friendly tracer gas helium is injected into the air flow. The ARR can be determined by measuring the reduction of the injected tracer occurring at the receiver front.

The goal was to achieve an ARR measurement with very high accuracy. This goal was reached as apparent from the very small minimal uncertainties of $\pm 0.5\,\%$.

So far the ARR of open volumetric receivers was often assumed and measured to be up to 60 % [14, 3]. The measured $ARR_{\mathrm{meas,dyn}}$ at the STJ of $(68.5 \pm 0.7)\,\%$ is higher than this expected value. Maldonado Quinto [8] has shown, that this difference corresponds to an increase of the expected overall system efficiency of $4-5\,\%$, making the open volumetric receiver concept more promising. The measurement performed under irradiation resulted in contrast to expectations in a slightly larger ARR.

Téllez et al. [12] measured a positive correlation between ARR and air mass flow. Although these measurements by Téllez et al. [12] should only be seen as a rough estimate, the ARR at the STJ is strongly dependent on the air mass flow and confirms this trend. The ARR without irradiation increased by 16 % when increasing the air mass flow from 5 kg/s to 10 kg/s. The ARR of an irradiated receiver increased by 12 % for the same air mass flow increase from 5 kg/s to 10 kg/s. These findings are based on four measurements only and can therefore not be separated from other sources of influence as for example wind.

8. Outlook

The ARR must be increased to improve the open volumetric receiver concept. Wind is suspected to have a significant influence on the ARR since losses due to $ARR < 1$ occur in front of the receiver. To allow correct annual efficiency predictions for potential power plant locations, knowledge of the influence of wind on the ARR is crucial, since the occurring wind speed differs strongly between locations. Especially for constructing power plants with taller tower heights, this is important as they are exposed to higher wind speeds. Therefore, the developed measurement techniques should henceforth be used to examine the influence of wind on the ARR.

The newly developed ARR measuring technique is currently be used to investigate the external air return system which was installed at the STJ. Hereby only a fraction of the returned air is blown out through the gaps between the absorbers. The separated fraction of the return air is brought in front of the receiver from the bottom and the sides. Maldonado Quinto [8] predicts from simulations an increase in the ARR to about 80 % for this external air return. The necessary ARR measurement to validate this have already been performed and will be covered within Stadler et al. [11].

Acknowledgements

This work was carried out with financial support from the Ministry of Innovation, Science and Research of the State of North Rhine-Westphalia (MIWF NRW), Germany under contract 323-2010-006 (Start-SF).

References

[1] Nils Ahlbrink, Joel Andersson, Moritz Diehl, and Robert Pitz-Paal. Optimization of the Mass Flow Rate Distribution of an Open Volumetric Air Receiver. *Journal of Solar Energy Engineering*, 135(4):041003, 2013. doi: 10.1115/1.4024245.

[2] Felix Andlauer. KAMs CSP Technology - an Economic and Highly Flexible Solution Designed for Full Market Integration, 8 2015. URL `http://www.ka-muenchen.de/fileadmin/Downloads_D/Broschueren/CSP_brochure_Web.pdf`.

[3] Antonio L Ávila-Marín. Volumetric receivers in solar thermal power plants with central receiver system technology: a review. *Solar Energy*, 85(5):891–910, 2011. URL `http://www.sciencedirect.com/science/article/pii/S0038092X11000302`.

[4] Edward Lansing Cussler. *Diffusion: mass transfer in fluid systems*. Cambridge university press, 2009.

[5] Karl-Heinz Funken. The Juelich Solar Power Tower, 2013. URL `http://www.dlr.de/sf/en/Portaldata/73/Resources/dokumente/grossanlagen/juelich/Juelich_Solar_Power_Tower-EN.pdf`.

[6] Bernhard Hoffschmidt, Felix M Tellez, Antonio Valverde, Jesus Fernandez, and Valerio Fernandez. Performance evaluation of the 200-kWth HiTRec-II open volumetric air receiver. *Journal of Solar Energy Engineering*, 125(1):87–94, 2003. doi: doi: 10.1115/1.1530627.

[7] Gerrit Koll, Peter Schwarzboezl, Klaus Hennecke, Thomas Hartz, Mark Schmitz, and Bernhard Hoffschmidt. The Solar Tower Juelich-a research and demonstration plant for central receiver systems. *Proceedings SolarPACES*, 2009. URL `http://elib.dlr.de/60306/`.

[8] Daniel Maldonado Quinto. *Konvektive Verluste an offenen volumetrischen Solarstrahlungsempfaengern*. PhD thesis, RWTH Aachen University, 2016.

[9] Manuel Romero and Aldo Steinfeld. Concentrating solar thermal power and thermochemical fuels. *Energy & Environmental Science*, 5(11):9234–9245, 2012. URL `http://dx.doi.org/10.1039/C2EE21275G`.

[10] Tobias Samus, Bastian Lang, and Holger Rohn. Assessing the natural resource use and the resource efficiency potential of

the Desertec concept. *Solar Energy*, 87:176–183, 2013. doi: doi:10.1016/j.solener.2012.10.011.

[11] Hannes Stadler, Arne Tiddens, Peter Schwarzbözl, Felix Göhring, and Torsten Baumann. Improved performance of open volumetric receivers by employing an external air return system. *Submitted to Solar Energy*, 2016.

[12] F Téllez, M. Romero, P. Heller, A. Valverde, J.F. Reche, S. Ulmer, and G Dibowski. Thermal Performance of "SolAir 3000 kWth" Ceramic Volumetric Solar Receiver. *12th International Symposium Solar Power and Chemical Energy Systems*, 2004. doi: doi:10.1016/j.solener.2011.02.002.

[13] Arne Tiddens, Marc Röger, Hannes Stadler, and Bernhard Hoffschmidt. A tracer gas leak rate measurement method for circular air circuits. *Flow Measurement and Instrumentation*, 47:45–53, 2016.

[14] Werner Vogel and Henry Kalb. *Large-scale solar thermal power: technologies, costs and development*. John Wiley & Sons, 2010.

[15] Henrik von Storch, Hannes Stadler, Martin Roeb, and Bernhard Hoffschmidt. Efficiency potential of indirectly heated solar reforming with open volumetric solar receiver. *Applied Thermal Engineering*, 2015. ISSN 1359-4311. URL `http://dx.doi.org/10.1016/j.applthermaleng.2015.05.026`.

Acronyms

ARR	air return ratio.
DLR	German aerospace center.
He	helium.
MS	mass spectrometer.
PIV	particle image velocimetry.
STJ	solar tower Juelich.